StonyBrook

State University of New York
at Stony Brook
Stony Brook, New York 11790

College of Engineering
Department of Materials Science
telephone: (516) 246-6759

AN INVESTIGATION OF PLASTIC FLOW IN CONSTRAINED COPPER CRYSTALS

by

Barry J. Berkowitz

U.S. Atomic Energy Research Contract No. AT-(11-1)-3476

Report No. COO-3476-5

SUSB 131 7-73

DISCLAIMER

AN INVESTIGATION OF PLASTIC FLOW IN CONSTRAINED COPPER CRYSTALS

A Thesis Presented

by

Barry Jay Berkowitz

to

The Graduate School

in partial fulfillment of the requirements

for the degree of

Master of Science

in

Materials Science

State University of New York

at

Stony Brook

June, 1973

STATE UNIVERSITY OF NEW YORK

AT STONY BROOK

THE GRADUATE SCHOOL

Barry J. Berkowitz

We, the thesis committee for the above candidate for the M.S. degree, hereby recommend acceptance of the thesis.

John C. Bilello
(Advisor and Chairman) John C. Bilello

Leslie L. Seigle Leslie L. Seigle

Patrick J. Herley Patrick J. Herley

Leslie L. Seigle
(Acting Chairman, Department of Materials Science) Leslie L. Seigle

The thesis is accepted by the Graduate School.

Dean, Graduate School

Abstract of the Thesis

AN INVESTIGATION OF PLASTIC FLOW
IN CONSTRAINED COPPER CRYSTALS

by

Barry Jay Berkowitz

Master of Science

in

Materials Science

State University of New York at Stony Brook

1973

Comparative studies of the changes in microstructure and micro-relaxation parameters were made between high purity copper single crystals and identical single crystals which had a surface modification. The latter specimens had a fine grain polycrystalline surface zone 20-40 microns thick, which was produced by controlled deformation and subsequent recrystallization. Such a zone meets the requirements of interface cohesion and is identical to the substrate in chemical composition and elastic parameters. Crystals with the surface zone exhibit a tripling of the yield stress and a Stage I work-hardening rate not much lower than that of Stage II. Relaxation data for modified crystals showed large recovered strains (about an order of magnitude larger than that

for single crystals) up to prestrains of 10^{-3}. Above this pre-strain the recovered strain was essentially the same as for copper single crystals in Stage I. Forest dislocation etch pit studies in conjunction with the above findings indicate that for constrained crystals, dislocations tend to be blocked below the coating-substrate interface. These dislocations cause stress concentrations (mostly due to screw dislocations), thereby playing a major role in producing an observed forest dislocation build-up. Some comparative studies were also made on copper plated single crystals.

TABLE OF CONTENTS

LIST OF FIGURES AND TABLES

ACKNOWLEDGMENTS

The author would like to express his appreciation to his advisor, Professor John C. Bilello, for his suggestions and valuable guidance throughout the progress of this thesis. Appreciation is also extended to John Dralla, Jan Pridans, and Samir Banerji for their help and suggestions. Thanks is also given to Mary-Faith Hughes for typing the manuscript. Finally, gratitude is extended to the Metallurgy and Materials Program of the United States Atomic Energy Commission for their financial support under Contract Number AT(11-1)-3476.

I. INTRODUCTION

The strengthening effect of coatings on single crystals is a well known phenomenon. Coatings produce plastic constraints to the substrate, thus limiting the mean free path for dislocation glide. The study of this behavior is essential; for a plastically constrained single crystal serves as an analog for polycrystals, multiphase alloys, composites and other constrained systems. In this study, mechanical testing and etch pitting techniques were employed to obtain information regarding the role of dislocations in copper single crystals and coated copper single crystals, It was found that plastic constraints cause an excess of dislocations in the substrate below the coating. This build-up of primary dislocations causes large stress concentrations (mostly due to screw dislocations) which result in an increase in the forest dislocation density.

Review of Previous Work

It has been shown that the surface plays a dominant role in the deformation process of face centered cubic metals. As an illustration of this, the work by Suzuki and coworkers (1) can be cited. They showed that there is a definite dependence of the termination of easy glide on the crystal diameter. The extent of easy glide must therefore be controlled in one way or

another by the presence of a surface region, for as a crystal diameter decreases, the ratio of surface region to bulk increases. Nakada and coworkers (2) further showed that the sample thickness in the direction parallel to the burgers vector has the most influence on the extent of easy glide, indicating that the interaction of dislocations with the surface region must be an important factor.

Fischer (3) postulated that the dislocation source generation stress should be lower nearer to the surface of a crystal. He explained that dislocations that penetrate the surface are relatively free to move at one end and effectively appear to be twice as long as the average interior dislocation source. Therefore, Frank-Read type dislocation sources at the surface should be capable of being activated at approximately one half the applied stress of an interior source. This was confirmed experimentally by Kitajima (4), Adams (5), Worzalla (6), and Latanision (7). More recently, Young and Sherrill (8), using x-ray Bormann topography were able to show dislocations moving in large numbers from the surface into the interior of the crystal during early stages of deformation.

Recently, the influence of the surface region on the deformation process has been discussed by Fourie (9, 10). He showed that the surface region of copper single crystals hardens more slowly than the interior during plastic deformation.

Fourie made these measurements in the unstressed state, and Mughrabi (11) confirmed these results by irradiating samples with neutrons, thereby pinning the dislocations in the stress applied state, and compared transmission electron micrographs of the surface region with the center of the crystal. The results showed that after Stage II deformation the dislocation density at the surface appears to still be characteristic of Stage I (easy glide). Mughrabi (12) further showed that as a result of this flow stress gradient, typical surface slip line data is not necessarily representative of the bulk during all stages of deformation and that an alternative formulation had to be derived.

In contrast to the above findings, Kramer and coworkers (13-21) suggest a debris layer model, whereby a crystal can have its original yield stress restored by chemically removing some of the surface. This effect was also shown by other workers (4, 22). The work hardening in crystals can then be explained, in terms of this model, by the accumulation of dislocations in surface debris zones which creates sufficient back stress opposing subsequent dislocation motion.

Fourie (23) likewise found that the removal of a surface envelope clearly reduces the yield point, but contrary to the debris layer model, he explains the phenomena simply as a result of a flow stress redistribution which occurs when a

crystal with a freshly exposed surface is further deformed.

There has been other contrasting results with regard to flow stress gradients and dislocation distributions. P.R. Swann (24) using electron microscope and Block and Johnson (25) using etch-pit techniques both found no dislocation density gradient after straining. On the other hand, Kitajima, Tanaka and Kaieda (26) showed by etch-pit studies that the primary dislocation density was higher in the surface region (50 - 100 microns) than in the bulk.

Another important influence of surface region on the mechanical behavior of metals occurs when a crystal is coated with a thin film. It was shown as early as 1936 by Roscoe (27) that a thin film of oxide on a cadmium single crystal caused an increase in the flow stress by a factor of about two, as compared to that of an uncoated crystal. This extraordinary effect was shown not to have been caused by the added shear strength of the film alone, and it was concluded that there must have been some unknown interaction between the film and the substrate.

Subsequently J.C. Fischer (3) in interpreting these results, extended his model by proposing that dislocation sources near the surface which normally operate at about half the shear stress as an interior source, are now inhibited due to a pinning of the normally free end of the dislocation at the film-substrate interface.

Many other workers have since proposed theories to explain this film strengthening phenomena. A.K. Head (28) has suggested an analogy between dislocations and electrostatic line charges. For films of higher elastic modulus than the substrate, the dislocations at large distances from the film are attracted to the surface while dislocations near to the film feel a short-range repulsive force. This theory was further elucidated by A.H. Cottrell (29) predicting an excess dislocation density near the film. C.S. Barrett (30-32) proposed a barrier effect whereby the mobile dislocations cannot leave the crystal during deformation due to the hard film. In uncoated crystals, the dislocations would leave the crystal at the surface, but a barrier prevents the dislocations from leaving and as a result high local dislocation densities should occur just below the film-substrate interface. Elbaum (33), Livingston and Chalmers (34) and Hausser and Chalmers (35) showed that the macroscopic incompatibility of grain boundaries results in multiple slip extenting large distances into the grain. Nakada and Chalmers (36) extend the above to suggest that the excess dislocation pile-up under the film causing stress concentrations which can only be relieved by means of secondary slip in the bulk. This causes enhanced dislocation interactions and therefore a substantial increase in the flow stress of coated crystals.

It has been suggested by Johnson and Block (37) that most of the observed film strengthening in chromium plated copper crystals can be attributed to cracks in the plating, which result in high local stress concentrations in the substrate. This was subsequently questioned by Bilello (38) based on calculations which showed that only a small percentage of the strengthening can be caused by this effect. It was later demonstrated by Pridans, Berkowitz and Bilello (39) that crystals with platings exhibit appreciable strengthening even though the platings were shown to be completely crack-free.

In a recent study of film strengthening, Pridans and Bilello (40) showed that the strengthening could be attributed to both short-range film repulsion plus a long-range interaction which extends deep into the bulk. It was suggested that this long-range interaction causes secondary slip activity to become more dominant throughout the bulk with increasing strain.

More recently, Livesay and Starke (41) studied the possible causes for film strengthening using extremely thin substrates and coatings (30 - 100 microns and 2200Å respectively) and found that the elastic modulus difference provided the primary strengthening mechanism for some FCC systems.

In other works, Patterson and Greenfield (42) showed how solid solution hardening at the surface caused strengthening in gold, and nickel diffused copper crystals. Also, Nakagawa

and Greenfield (43) studied silver diffused copper explaining strengthening in terms of a high density of sessile misfit dislocations near the interface.

Analysis of the Recent Literature

There have been two kinds of arguments to explain the role of surfaces in the deformation processes of FCC metals. Some workers (9-12) showed that during deformation of copper single crystals, the surface of the crystal seemed to deform slower than the interior and that the dislocation density at the surface was very much lower than that of the bulk after a few percent strain.

On the other hand, other experiments on copper crystals (13-21) showed contrasting results, i.e. after deformation the dislocation density was found to be higher at the surface.

The reason for the disparity probably lies in the method of crystal preparation. It should be noted that all of the workers (13-21) that found a hardened surface zone prepared their crystals using modified Bridgman techniques involving hard graphite or porcelain molds, while experiments which revealed a soft surface region (9-12) used either an open boat growth technique or a soft powdered graphite mold method. One possible explanation may be that the observed differences are due primarily to the initial structure, for a crystal with

constricted surfaces during growth would seem to have a higher initial dislocation density at the surface while one with free surfaces would exhibit a more uniform initial structure. This certainly could give rise to the aforementioned differences in dislocation structures of strained crystals. Therefore, great care was taken in the present experiments to compare results only to known initial dislocation structures.

Experimental Plan

In view of past work, the present experiments were planned to observe the influence of a constrained single crystal, with as far as possible, no other intervening effects present i.e. excluding modulus differences, interface non-cohesion, surface energy differences, surface zone solid solutions, etc. It was felt that a new approach was needed to do this. In the past, workers have used plated or sputtered film techniques as a means of studying surface effects, but the problems with films are that they are not necessarily cohesive with the substrate and may crack or even disengage. Instead, inherent polycrystalline surface layers were produced by extending the methods developed by others for zinc and tin (44, 45).

In this study a modified single crystal was developed with a very fine grained, inherent, polycrystalline surface region. This new completely cohesive surface of identical

material and elastic constants was then employed to explore the deformation processes in normal single crystals.

The most important tool for this study was a tensile testing machine. From the load-elongation data, information concerning the comparisons of modified and normal single crystals were obtained. Relaxation information, which gave new insight into possible deformation mechanisms, was also gathered.

Etch pit data was also obtained in order to better characterize the role that both edge and screw dislocations play in the deformation process for coated and uncoated crystals.

II. EXPERIMENTAL PROCEDURE

Crystal Preparation

A modified Bridgman Technique was used to grow single crystals from ASARCO 99.999% pure copper. A Synchronous motor provided a growth rate of 5 cm/hour which has been shown (46) to give a good balance between subgrain size and dislocation density. The crystals were grown in two-track (5mm x 5mm each) graphite molds in vacuum better than 1×10^{-5} Torr. The crystals produced were each about 20 cm long grown from seeds oriented at 3^{o} from (001) with a pair of faces $\sim 1^{o}$ from {111}. The crystals were then sectioned into 5 cm long samples using a modified acid saw technique (47) and polished in a 60% Ortho-phosphoric acid solution to make the faces smooth enough for etching purposes. All of the samples were then annealed in vacuum better than 1×10^{-5} Torr at 1050^{o}C for eight days. The initial dislocation densities of all the samples were between 1×10^{5} and 1×10^{6} cm/cm^{3}.

Some of the samples were then modified as follows: a sample was placed in wax in a holder and stroked under a controlled contact stress across a 320 grit paper to produce deformation only at the surfaces. This procedure damaged a zone only $\sim$ 20-40 microns into the bulk leaving the remainder of the crystal unaffected (as observed by sectioning and etch pitting). The

crystal was then removed from the holder and wax and was annealed at 450°C for thirty minutes so that the surface of the crystal recrystallized with a final grain size at the surface of about 10 to 20 μm. After polishing 40 μm into the crystal, all the grains were removed leaving the original single crystal.

In order to determine the depth and characteristics of this surface zone, a sample was first sectioned and photographed (shown in Fig. 1a), in order to determine the depth of the surface layer. Next, the surface was etched (Fig. 1b) which illustrated the grain size of the surface. Lastly, the sample was x-rayed producing a Laue photograph (Fig. 1c). The rings produced indicate that the surface zone is not highly textured. The bright spots are reflections from the substrate (the depth of penetration of the x-rays is greater than the thickness of the surface coating).

Mechanical Testing

The samples were mounted into self-aligning ball joint grips using a creep-resistant soft solder. During soldering, the sample and grips were held in place by a lavite alignment jig to insure accuracy. The samples were mechanically tested on a Table Model Instron Tensile Testing Machine at a strain rate of $\approx 1.67 \times 10^{-4} \text{sec.}^{-1}$. A standard prestress of 4 gm/mm^2 was used for the purpose of initial alignments. The

load-displacement data was directly plotted using an x-y plotter. The y-channel of the plotter recorded the information from the load cell while the x-channel recorded the information from linear variable differential transducers (LVDT) which were incorporated directly in the sample grips thereby measuring only the instantaneous elongation of the sample.

All tests were done at room temperature at strain sensitivities $\gtrsim 1 \times 10^{-6}$. So that temperature fluctuations would not affect the relaxation results, a styrofoam shielding was used to keep the sample temperature constant.

To obtain high sensitivity strain relaxation data at relatively large prestrains, zero suppression capable of suppressing prestrains up to approximately 10^{-2} had to be used to keep the data on the graph. The zero suppression instrument was built directly into the Daytronic amplifier which amplified the signals from the LVDT.

Etch Pitting Techniques

Livingston's (48) etch was used to reveal dislocations on both primary and forest {111} planes. Acid cut surfaces were prepared for etching by using an acid wheel polisher (49) using the polishing technique of Mitchell, et al. (50), to flatten the surface with very little or no mechanical damage and then electropolish to smoothen the surface to be etched.

After a given amount of prestrain, in order to etch a particular (111) plane, the sample was first unsoldered from its grips and then x-rayed to determine the angle at which it had to be cut. The sample was then set in a lucite track on a goniometer stage of the acid saw. String tension and acid flow were continuously monitored so as to produce as flat a cut as possible. Next, the sample was placed in a wax mount with the cut face exposed. The wax was then affixed to the holder of the wheel polisher and the sample was slowly adjusted closer and closer to the wheel using a cathetometer until the polishing solution on the wheel formed a capillary bridge. The surface tension of the liquid maintained this bridge as the wheel rotated. To avoid rounding of the edges of the sample, a 10 micron layer of copper was plated to the sides of the sample using a technique reported by Pickus and Parker (51) and then a thin layer of microstop was applied on top of the plating. This procedure kept the sample flat to within 10 microns of the edge. The sample was then electropolished in 60% Orthophosphoric acid producing a very flat, shiny surface which was then suitable for etching.

III. RESULTS

Stress-Strain Behavior - General Features

All samples were tested using a uniform procedure (see Fig. 2). Each sample was loaded and unloaded in increments of strain such that there were about four or five loops for each cycle of prestrain on a logarithmic scale. The figure shows one typical loop of resolved shear stress vs. resolved shear strain for the purpose of identifying various characteristics of the deformation behavior.

For the uncoated single crystals there is an initial linear region, (i), terminating at the stress τ_E. The stress τ_E is actually the anelastic limit rather than the elastic limit because preliminary tests on previously unstrained crystals showed no loop retracing for any detectable stress limit. It has been shown (52) that the microyield stress for very pure copper single crystals is in the neighborhood of 2 gm/mm^2. The elastic limit is therefore below the level of prestress ($\sim$ 4 gm/mm^2) used for alignment.

While the crystal is straining in the flow region, the crosshead motion is reversed at stress τ_m, the maximum loop stress. The unloading behavior is initially linear with approximately the same slope as region "i". At a stress τ_u the crystal begins to plastically relax. This relaxation continues until zero stress

is reached (excluding prestress) at which point a total amount of plastic strain, a_r, is recovered and a permanent plastic strain, Δa, remains.

The behavior of crystals with inherent polycrystalline surface regions are similar in character except that τ_E is the stress level below which loop retracing occurs. Above τ_E there is another linear region, "ii", of smaller slope, continuing to τ_p, the anelastic limit. There is only one detectable linear region during unloading for all crystals.

Crystals that were electroplated with thirty microns of copper showed only one detectable linear region during loading.

Proportional Limits and Slopes

The proportional limits of both coated and uncoated crystals are shown in Fig. 3. It is noted that the proportional limits of samples 4d and 4e (single crystals) are fairly constant, those of 3c (crystal with inherent polycrystalline surface) vary greatly. τ_E of 3c gradually decreases until region "i" eventually disappears at a strain $\approx 10^{-3}$. τ_p of 3c shows an initial rise until a strain of $\approx 10^{-4}$ and then also shows a decreasing trend.

Fig. 4 shows the relative slopes of the initial linear regions of the deformation behavior of various crystals. The plots indicate the percent deviation from the theoretical calculation of Young's Modulus, E, for this orientation (53).

Samples 4d and 4e show fairly high deviations indicating that their initial linear regions are indeed exhibiting anelasticity. Crystal 3c shows two regions of anelasticity, regions "i", and "ii". It should be noted that the slope of region "i" is constant even though τ_E steadily decreases.

Strain Relaxation Behavior

Recovered strain vs. accumulated prestrain is plotted in Fig. 5. Samples 4d and 4e (single crystals) show two linear regions on a log-log plot with the change in slope at about 7 or 8% strain. Samples 3c and 3e (polycrystalline surface) exhibit recovered strains of almost an order of magnitude higher than that of the single crystals to a strain $\approx 2 \times 10^{-3}$. In both 3c and 3e the recovered strains continually rise, reach a local peak, and then level off to a constant slope not very much different from that of the single crystals. Sample 3g (30 micron plating) shows three distinct regions of constant slope, the first ending at $\approx 5 \times 10^{-3}$ and the second at $\approx 1 \times 10^{-2}$.

Macrostress-Strain Behavior

The macrostress-strain curves of various crystals are shown in Fig. 6. The most obvious aspect of the curves is that the yield stress, τ_{ys}, determined as the Stage I flow stress extrapolated to zero strain (see Fig. 2), for the inherent

polycrystalline coated samples (3c and 3e) are about three times greater than that of the single crystals (3d, 4d, and 4e). Also, 4d and 4e show easy glide until about 5 and 7 percent respectively, while 3c shows approximately the same Stage I-II transition, but has a much higher Stage I work hardening rate, θ_I (not much different from Stage II for 3c). The Stage I-II transition is indicated on Fig. 6 as "a(I-II)". It is also noted that the work hardening rates of all crystals during Stage II, θ_{II}, are approximately the same. Sample 3g (plated) shows a hybridization of the behavior of both single crystals and crystals with inherent polycrystalline surface regions. Below a strain of 5×10^{-3}, 3g appears to be similar in character to 3d, but above this strain it more resembles the behavior of 3c.

Samples 3d and 3e were strained only to 2% and sectioned for etch pit studies.

The yield stress, work hardening rates, and Stage I-II transition strains of various crystals are shown in Table 1.

Forest Dislocation Densities and Distributions

Fig. 7 shows a composite photograph of forest dislocation etch pits revealed on the primary plane (111) of 3e after 2% strain. The intersection of the primary slip plane with the $(11\bar{1})$ side face is visible at the bottom of the photograph. Composite photographs were used to extract the forest dislocation density

Table 1. Summary of Stress-Strain Data

Crystal	Description	τ_{ys}	θ_I	θ_{II}	a(I-II)
3c	polycrystalline surface	0.33 kg/mm^2	8.8 kg/mm^2	11.7 kg/mm^2	5.6%
3d	normal	0.11	4.3	———	———
3e	polycrystalline surface	0.34	4.4	———	———
3g	plated	0.12	9.2	11.7	6.0
4d	normal	0.09	3.9	11.3	5.4
4e	normal	0.08	3.2	10.4	7.6

as a function of depth into the crystal for single crystal 3d and polycrystalline coated crystal 3e. Etch pits were counted in various areas, giving statistically representative data. This information is plotted in Fig. 8.

For each crystal, the log of the dislocation density is plotted as a function of distance from two adjacent side faces of the crystal i.e. $(11\bar{1})$ side face and $(2\bar{1}1)$ side face. It should be noted that the forest densities as measured from both surfaces of both crystals are generally the same in the bulk, but are greater near the side surfaces of sample 3e. Also, the high density of the $(11\bar{1})$ surface of 3e extends much further into the bulk than that of 3d, while this effect is not prominent for the $(2\bar{1}1)$ surface.

IV. DISCUSSION

Physical Interpretation of Dislocation Recovery

The total recovered strain due to all the relaxing dislocations is given as:

$$a_r = N_r \bar{D}_r b$$

where N_r is the total of mobile dislocations in the reverse direction, and $\bar{D}_r$ is the average distance that these dislocations recover. The strain relaxation behavior (Fig. 5) of the single crystals increases steadily as a function of strain (to $\sim$ 7%), indicating that the product $N_r \bar{D}_r$ is also steadily increasing. At point "a(I-II)", the recovered strains of the single crystal show a sharp increase with increasing strain indicating that the $N_r \bar{D}_r$ increases more rapidly at the onset of Stage II behavior.

Crystals with inherent polycrystalline surface layers show strain relaxation curves whose behavior can be explained as follows: at small strains (to $\sim 10^{-3}$), the amount of recovery is relatively high because dislocations in the crystal cannot pass through the elastic polycrystalline surface region. The dislocations pile-up, in a sense, against the unyielding surface, and when the applied stress is relieved, large back stresses cause the dislocations to move in the reverse direction. Uncoated crystals should exhibit smaller relaxations, because the

dislocations on the glide plane easily form a step at the surface thereby eliminating the stress field associated with the dislocation.

At the local peaks in the relaxation curves for 3c and 3e it is believed that the polycrystalline surface begins to yield. At this point, the amount of recovery per unit strain begins to level off, because the dislocation strain fields can now be relieved at the polycrystalline-substrate interface. Above $\gtrsim 3 \times 10^{-3}$ strain, the slopes for these curves resembles those for the single crystals, and it should be noted on the stress-strain curve (Fig. 6) that the crystals are still showing Stage I behavior. Evidently, this relaxation region of constant slope is indicative of easy glide, i.e. $N\overline{D}$ (for forward motion) and $N_r\overline{D}_r$ are both increasing steadily in this region.

The plated copper crystal shows a behavior that is characteristic of both the single crystals and the crystals with the polycrystalline surface layers. To strains of $\gtrsim 5 \times 10^{-3}$ both the stress-strain and relaxation behavior is reminiscent of the single crystals. This is most likely due to inhomogeneous yielding of the crystal at the few points where the film might have decohered or disengaged. At higher strains, the deformation becomes more homogeneous and these finite areas become exhausted so that most of the dislocations now see a cohesive coating similar to the polycrystalline layer of 3c and 3e. The stress-strain

curve as well as the strain relaxation curve of 3g (plated) shows a rapid increase to strains $\gtrsim$ 1% at which point, the slopes of both curves take on the qualities of the curves of the other crystals in Stage I.

Even though the relative slopes in the easy glide region of all crystals are similar, the magnitudes vary over a wide range. This can be explained in terms of the grain size of the surface region. The uncoated crystals exhibit the least amount of recovery in this region because of the relatively free surface. Most dislocations can egress at the surface, thereby relieving the back stresses. The plated crystal shows the highest recovery, because the very fine grains, indicative of electroplatings, yield at much higher stresses than that of the inherent polycrystalline layer (grain size $\gtrsim$ 10-20 microns). It is therefore more likely that a plating would provide the most plastic constraint (assuming cohesion), thereby increasing the amount of recovery of near surface dislocations.

The Role of Screw Dislocations During Deformation

The dislocation forest density after 2% strain of single crystal 3d and polycrystalline surfaced crystal 3e is shown as a function of depth from the side surfaces (Fig. 8). The forest density in the bulk seems to be independent of the kind of surface to 2%, but the forest density for the coated approaches a

higher value at the surface than that of the uncoated. Also note that the densities as a function of depth from the $(2\bar{1}1)$ side face for both crystals are about the same, but the densities as a function of depth from the $(11\bar{1})$ side face shows much higher values for the coated crystal.

The reason for this behavior is that the dislocations that approach the $(11\bar{1})$ side face during deformation are screw in character, while those approaching the $(2\bar{1}1)$ face are mostly edge in nature. Hauser and Chalmers (54) in dealing with plastic constraints produced by incompatible boundaries show that the unrelaxed stress due to screw dislocation pile-ups is more pronounced and extends deeper into the crystal than that of edge dislocations.

The increase in the forest density at the surface is thus a manifestation of the stress concentrations at the boundary that must be relieved. It is reasonable to assume that the initially high relaxation data of the polycrystalline coated crystal is due to this unrelaxed stress, i.e. the aforementioned back stress, and that the screw dislocations must therefore be the major contributors in the work-hardening process.

The recent finds of Nakagawa and Greenfield (43) seem to be consistent with the above. After diffusing silver into surface layers of copper of orientations (001) and (110), it was found that the (001) surface orientation exhibited the greatest

hardening. It was argued that this hardening is due to misfit dislocations accomodating the diffused silver layer. The (001) diffusion zone contains sessile edge dislocations, while the (110) contains sessile edge and glissile mixed dislocations. Under an applied stress, the difference in strengthening was explained in terms of a blocking effect by the sessile edge dislocations.

It should be pointed out though that during deformation, mostly screw dislocations approach the (001) surface, while an abundance of edge dislocations approach the (110) surface. The phenomenon may then be explained as the blocking of the egress of the screw dislocations causing the high stress concentrations discussed earlier.

In summary, the present work showed that for uncoated single crystals where dislocations can egress at the free surface, the internal stresses can be relieved without building up large constraints. For crystals with barriers, such as coatings or grain boundaries, dislocations tend to be blocked and nucleate secondary slip, with primary screw dislocation segments playing the major role in producing the resultant forest dislocation build-up.

REFERENCES

1. Suzuki, H., Ikeda, S., and Takeuchi, S.; J. Phys. Soc. Japan, 11, 382 (1956).

2. Nakada, Y., Kochs, U.F., and Chalmers, B.; Trans. MS AIME, 230, 1273 (1964).

3. Fischer, J.C.; Trans. MS AIME, 194, 531 (1952).

4. Kitajima, S., Oasa, H., and Kaieda, H.; Trans. Japan Inst. of Metals, 8, 185 (1967).

5. Adams, M.A.; Acta Met., 6, 327 (1958).

6. Worzala, F.J., and Robinson, W.H.; Acta Met., 17, 307 (1969).

7. Latanision, R.M., and Staehle; R.W., Acta Met., 17, 307, (1969).

8. Young, F.W., Jr., and Sherrill, F.A.; Can. J. Phys., 45, 757 (1967).

9. Fourie, J.T.; Can. J. Phys., 45, 777 (1967).

10. Fourie, J.T.; Phil. Mag., 17, 735 (1968).

11. Mughrabi, H; Phys. Stats. Sol., 39, 317 (1970).

12. Mughrabi, H.; Phys. Stats. Sol., 44, 391 (1971).

13. Kramer, J.R., and Demer, L.J.; Trans. MS AIME, 221, 780 (1961).

14. Kramer, J.R.; Trans. MS AIME, 221, 989 (1961).

15. Kramer, J.R.; Trans. MS AIME, 227, 529 (1963).

16. Kramer, J.R.; Trans. MS AIME, 227, 1003 (1963).

17. Kramer, J.R.; Trans. MS AIME, 230, 991 (1964).

18. Kramer, J.R.; Trans. MS AIME, 233, 1462 (1965).

19. Feng, C., and Kramer, J.R., Trans. MS AIME, 233, 1467 (1965).

20. Kramer, J.R., and Aehner, C.L.; Acta Met., 15, 678 (1967).

21. Kramer, J.R., and Kumar, A.; Scripta Met., 3, 205 (1969).

22. Cansey, A.R., and Teghtsoonian, E.; Trans. MS AIME, 223, 1920 (1965).

23. Fourie, J.T.; Phil. Mag., 22, 923 (1970).

24. Swann, P.R.; Acta Met., 14, 900 (1966).

25. Block, R.J., and Johnson, R.M.; Acta Met., 17, 299 (1969).

26. Kitajima, S., Tanaka, H., and Kaieda, H.; Trans. Japan Inst. of Metals, 10, 12 (1968).

27. Roscoe, R., Phil. Mag.; 21, 399 (1936).

28. Head, A.K.; Phil. Mag., 44, 92 (1953).

29. Cottrell, A.K.; Dislocations and Plastic Flow in Crystals, Oxford:Clarendon Press (1953) p. 55.

30. Barrett, C.S.; Acta Met., 1, 2 (1953).

31. Barrett, C.S., Aziz, P.M., and Markson, I.; Trans. MS AIME, 197, 1655 (1953).

32. Barrett, C.S.; Trans. MS AIME, 197, 1652 (1953).

33. Elbaum, C.; Trans. MS AIME, 218, 444 (1960).

34. Livingston, J.D., and Chalmers, B.; Acta Met., 5, 322 (1957).

35. Hauser, J.J., and Chalmers, B.; Acta Met., 9, 802 (1961).

36. Nakada, Y. and Chalmers, B.; Trans. MS AIME, 230, 1339 (1964).

37. Johnson, R.M., and Block, R.J.; Acta Met., 16, 831 (1968).

38. Bilello, J.C.; Scripta Met., 4, 493 (1970).

39. Pridans, J., Berkowitz, B.J., and Bilello, J.C.; Scripta Met., 5, 701 (1971).

40. Pridans, J. and BIlello, J.C.; Acta Met., 20, 1339 (1972).

41. Livesay, B.R. and Stark, E.A., Jr.; Acta Met., 21, 247 (1973).

42. Patterson, W.R. and Greenfield, I.G.; Acta Met., 19, 123 (1971).

43. Nakagawa, Y.G. and Greenfield, J.G.; Acta Met., 21, 367 (1973).

44. Galligan, J.M. and Feuerstein, S.; Trans. MS AIME, 233, 263, (1965).

45. Causey, A.R., and Teghtsoonian, E.; Trans. MS AIME, 233, 1920 (1965).

46. Evans, K.R. and Flanagan, W.F.; Phil. Mag., 14, 1131 (1966).

47. Armstrong, R.W., and Rapp, R.A.; Rev. Sci. Instrum., 29, 433 (1958).

48. Livingston, J.D.; J. Appl. Phys., 31, 1071 (1960).

49. Young, F.W., and Wilson, T.R.; Rev. Sci. Instrum., 32, 559, (1961).

50. Mitchell, J.W., Chevrier, J.C., Hockey, B.J., and Monaghan, J.P., Jr.; Can. J. Phys., 45, 453 (1967).

51. Pickus, M.R., and Parker, E.R.; Trans. MS AIME, 191, 792 (1951).

52. Tinder, R.F. and Washburn, J.; Acta Met., 12, 129 (1964).

53. Schmid, E. and Boas, W.; Plasticity of Crystals, London: Chapman and Hall, Ltd. (1950) pp. 20-21.

54. Hauser, J.J., and Chalmers, B., Acta Met., 9, 802 (1961).

Fig. 1.

(a) Sectioned copper crystal with inherent polycrystalline surface

(b) Micrograph of the inherent polycrystalline surface after etching

(c) Laue photograph of the inherent polycrystalline surface showing no obvious texture

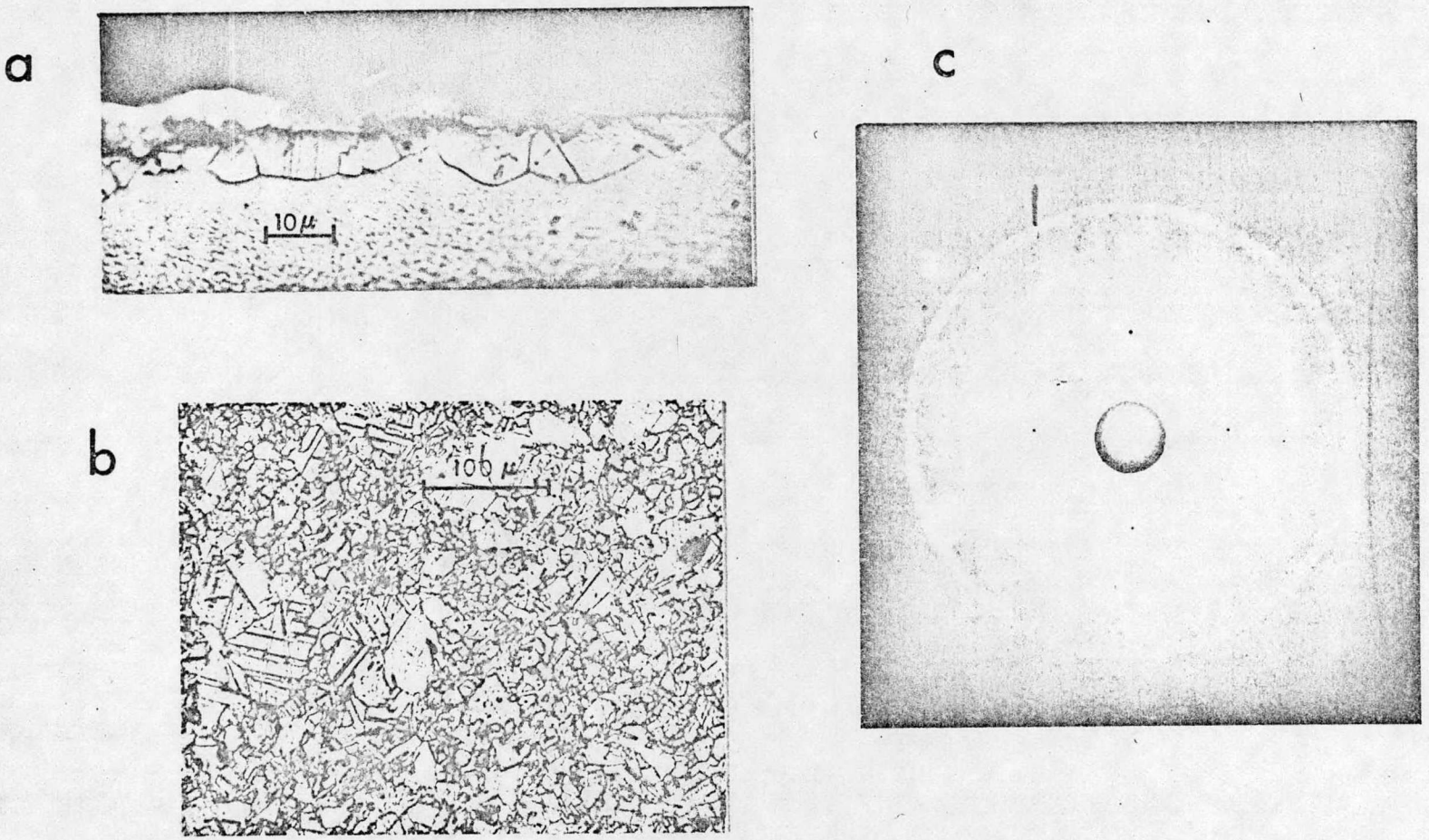

Fig. 1

Fig. 2. Typical stress-strain loop showing the various micro-relaxation parameters.

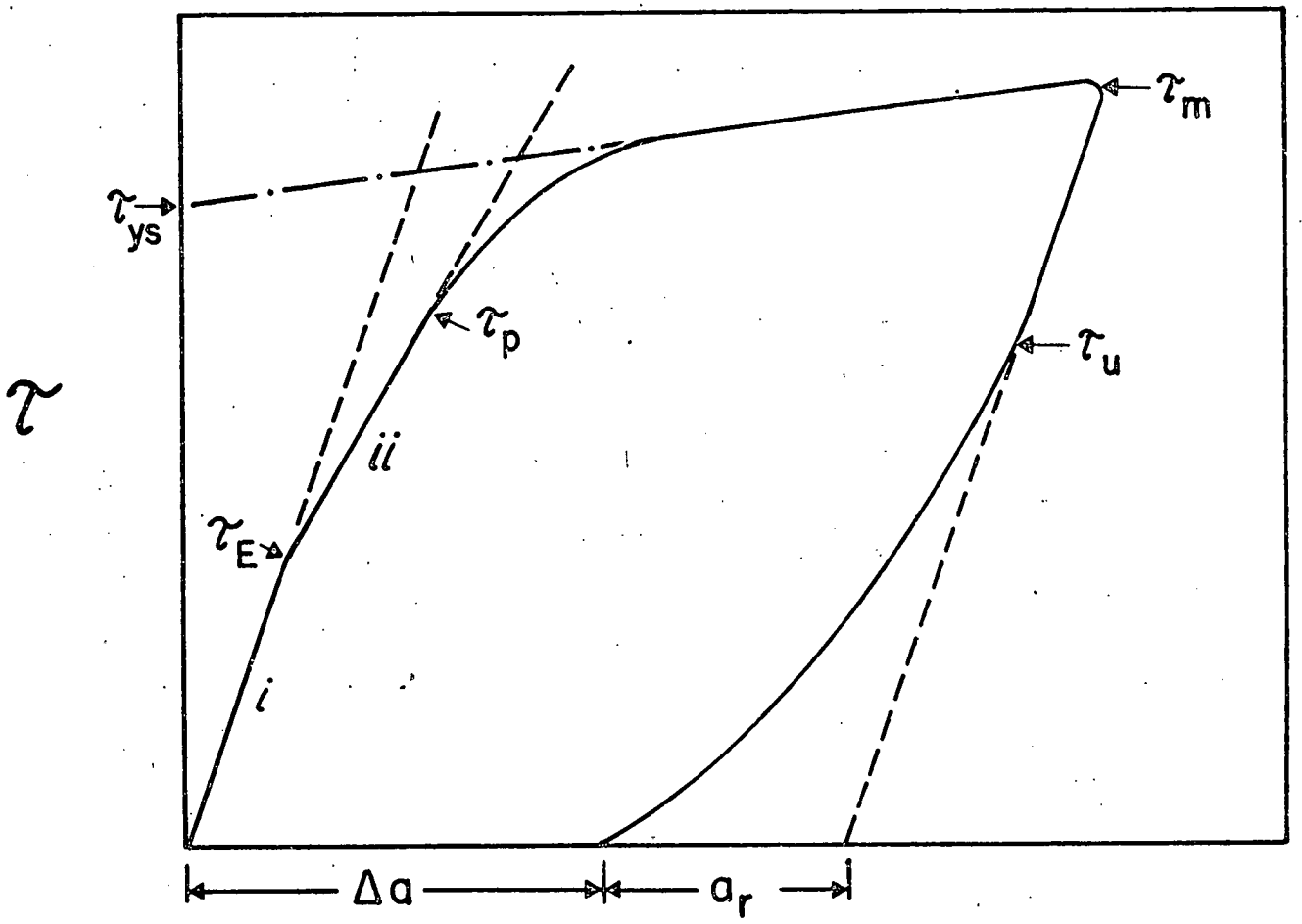

Fig. 2

Fig. 3. The proportional (resolved shear stress) limits vs. resolved shear strain of the initial linear regions of both single crystals and crystals with inherent polycrystalline surface layers.

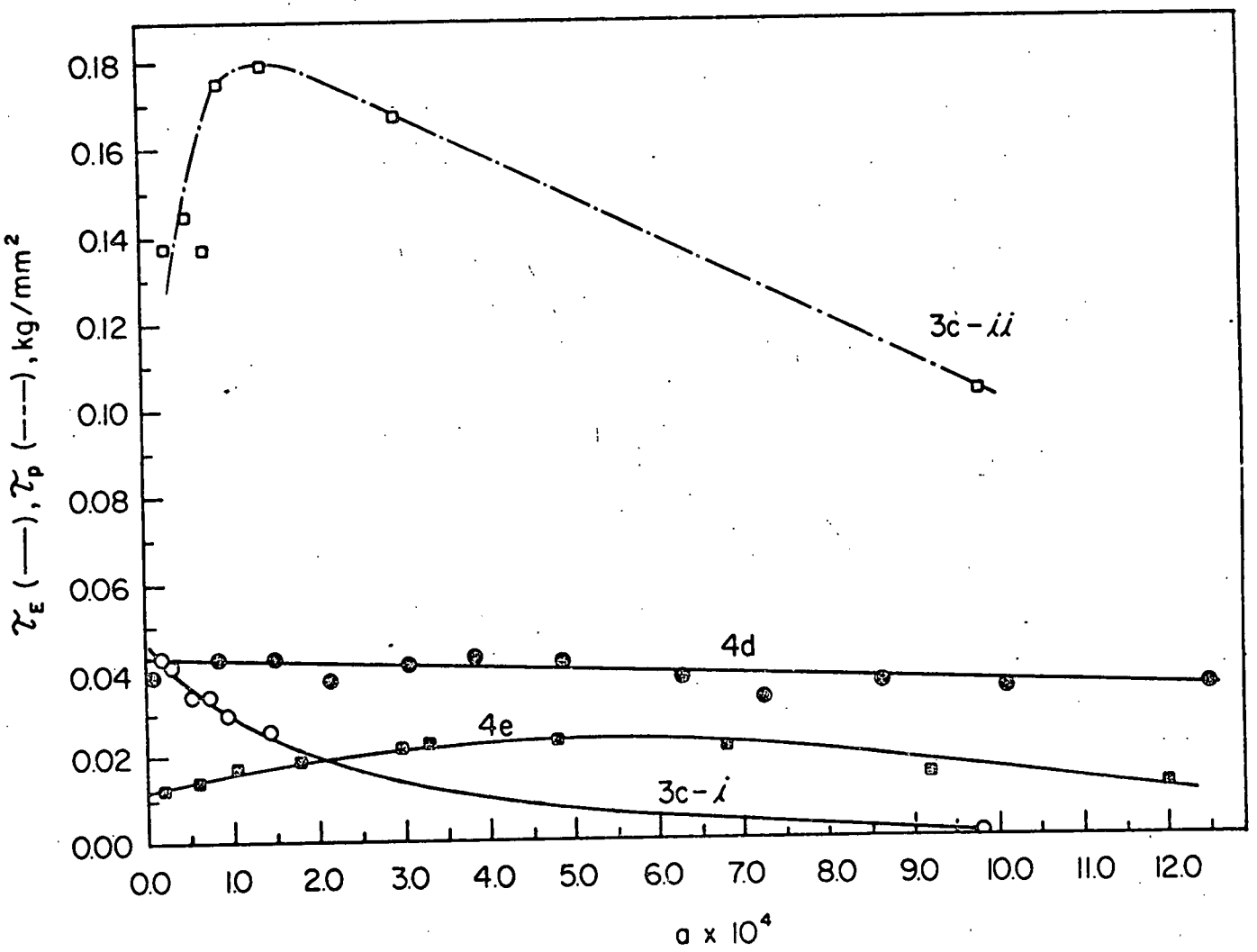
0.18
0.16
0.14
0.12
0.10
0.08
0.06
0.04
0.02
0.00
τ_ε (——), τ_p (– – –), kg/mm²
3c – ii
4d
4e
3c – i
0.0
1.0
2.0
3.0
4.0
5.0
6.0
7.0
8.0
9.0
10.0
11.0
12.0
a x 10⁴

Fig. 3

Fig. 4. The % modulus reduction vs. resolved shear strain for single crystals and crystals with inherent poly-crystalline surface layers.

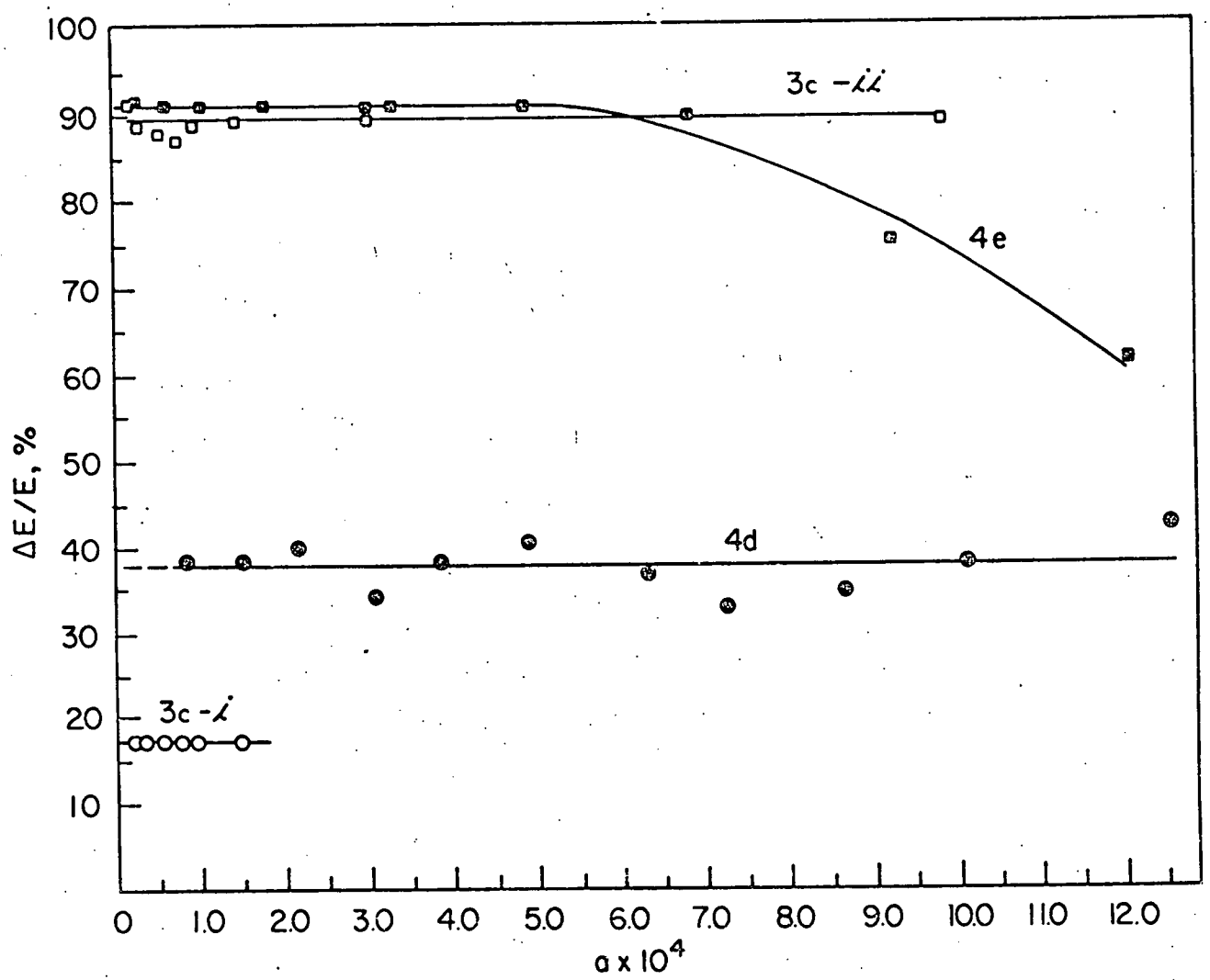
100
90
80
70
60
50
40
30
20
10
ΔE/E, %
3c -ii
4e
4d
3c -i
0
1.0
2.0
3.0
4.0
5.0
6.0
7.0
8.0
9.0
10.0
11.0
12.0
a x 10^4

Fig. 4

Fig. 5. Recovered resolved shear strain vs. resolved shear strain for coated and uncoated crystals.

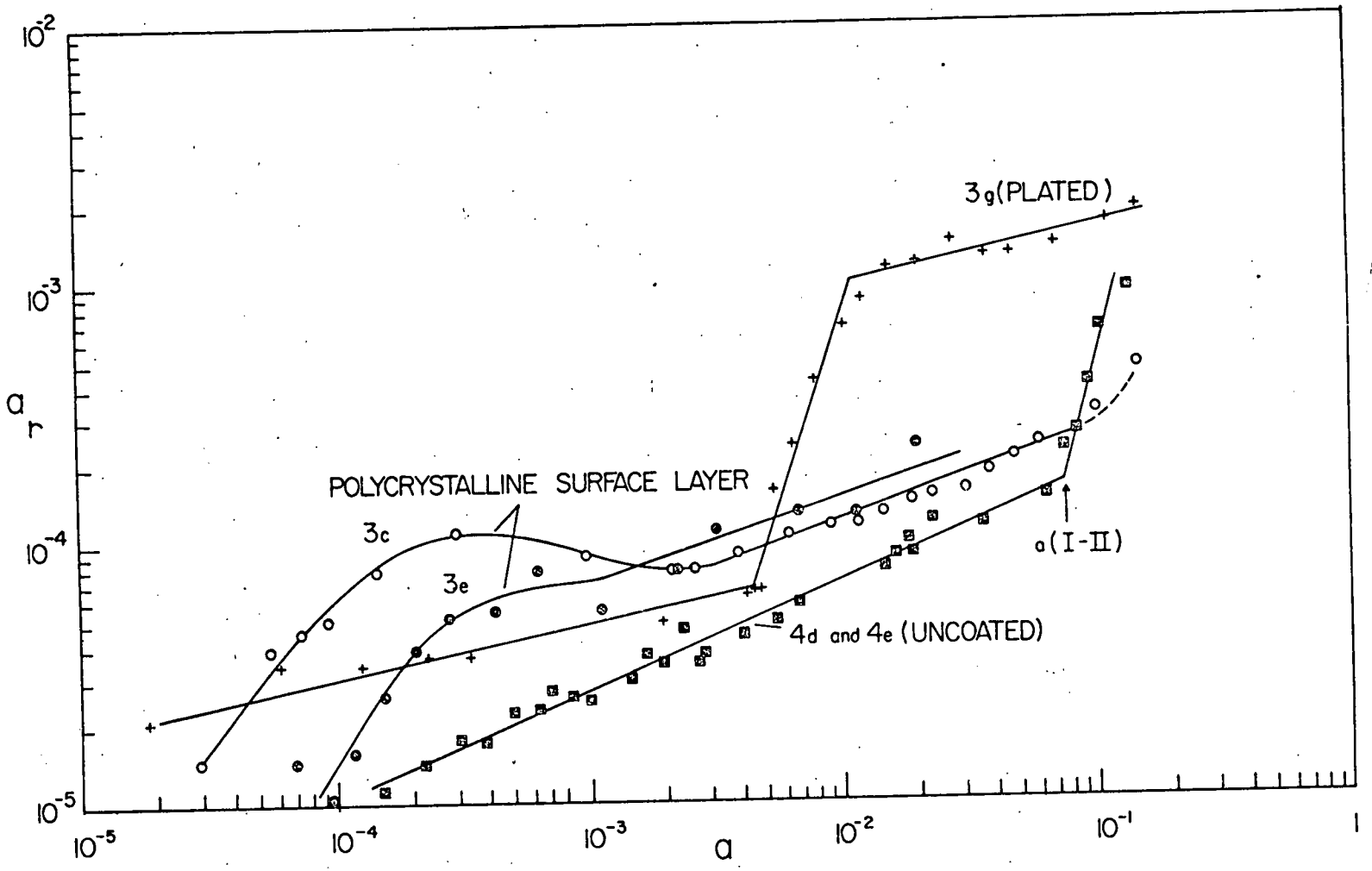
10^{-2}
10^{-3}
10^{-4}
10^{-5}
a_r
10^{-5}
10^{-4}
10^{-3}
10^{-2}
10^{-1}
1
a
3g(PLATED)
POLYCRYSTALLINE SURFACE LAYER
3c
3e
4d and 4e (UNCOATED)
a(I-II)

FIG 5

Fig. 6. Resolved shear stress vs. resolved shear strain for various coated and uncoated crystals.

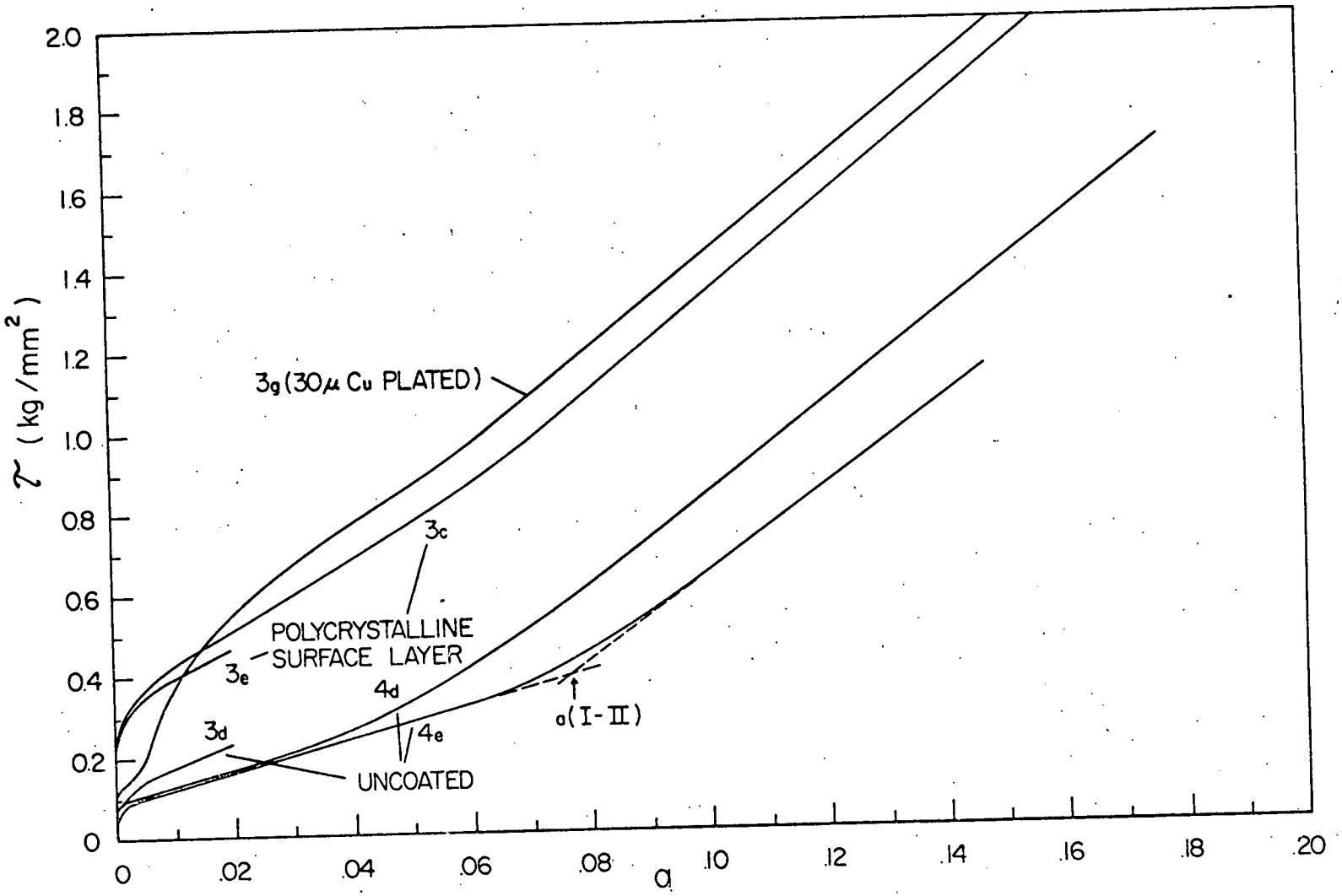
2.0
1.8
1.6
1.4
1.2
1.0
0.8
0.6
0.4
0.2
0
τ (kg/mm²)
3g (30μ Cu PLATED)
3c
POLYCRYSTALLINE
SURFACE LAYER
3e
4d
3d
4e
UNCOATED
α(I-II)
0
.02
.04
.06
.08
.10
.12
.14
.16
.18
.20
α

FIG 6

Fig. 7. Composite photomicrograph of the (111) plane etched to reveal dislocations.

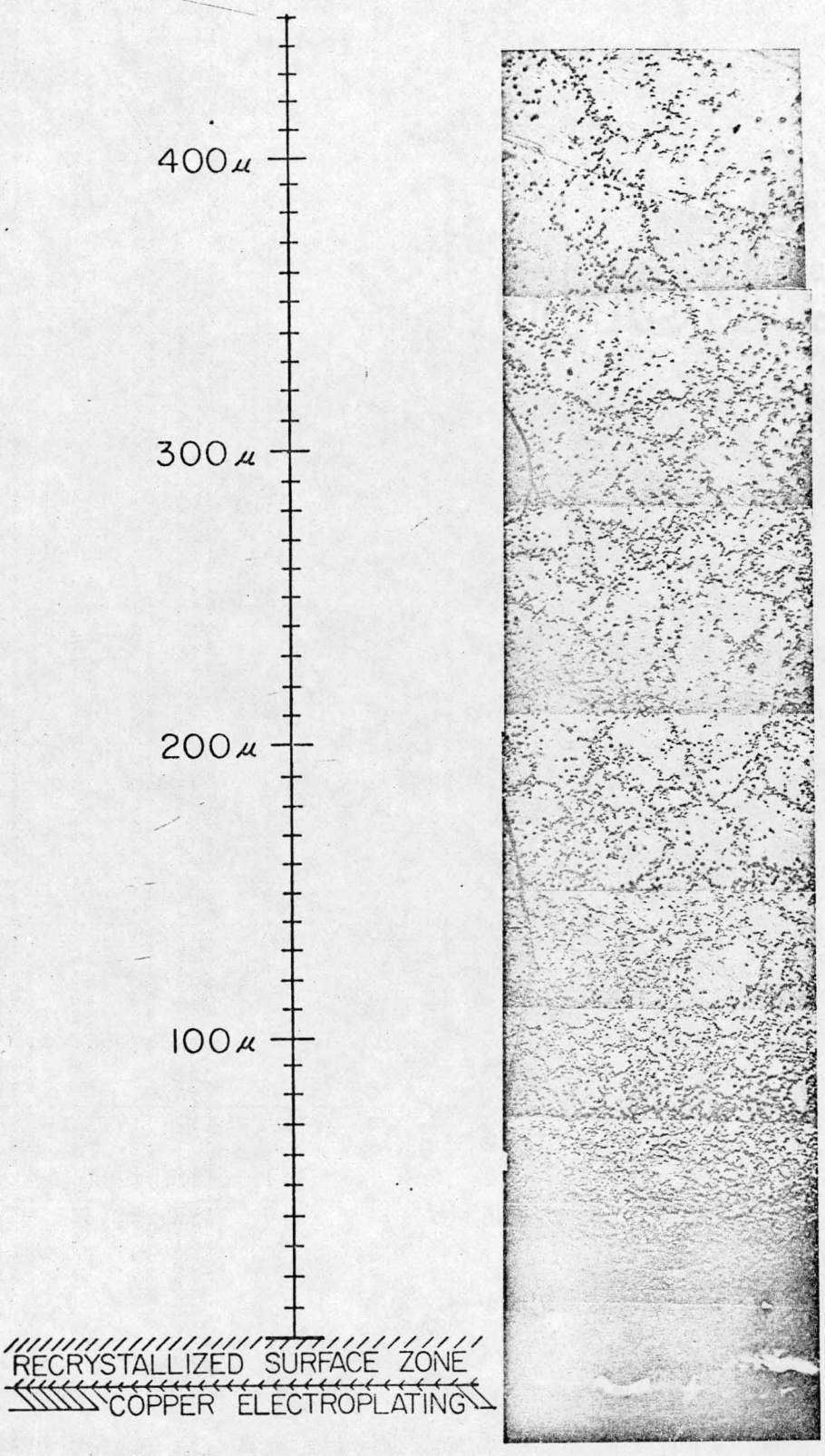
400 μ
300 μ
200 μ
100 μ
RECRYSTALLIZED SURFACE ZONE
COPPER ELECTROPLATING

Fig. 7

Fig. 8. Forest dislocation density as a function of depth into the crystal
from $(11\bar{1})$ side face of 3d ●
from $(2\bar{1}1)$ side face of 3d ■
from $(11\bar{1})$ side face of 3e ○
from $(2\bar{1}1)$ side face of 3e □

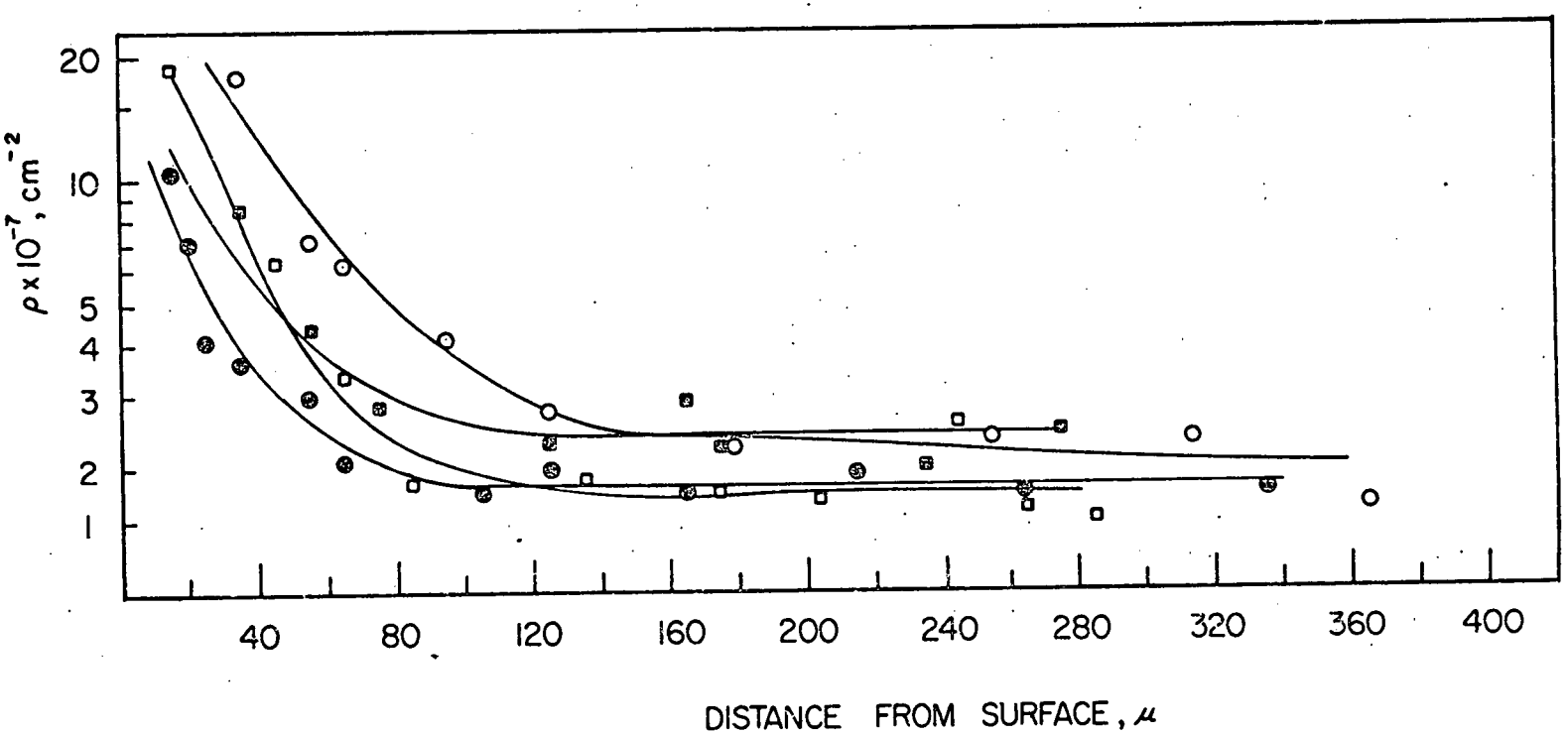
20
10
5
4
3
2
1
$\rho \times 10^{-7}, cm^{-2}$
40
80
120
160
200
240
280
320
360
400
DISTANCE FROM SURFACE, μ

Fig. 8